ANL/NSE-25/31

Benchmark Exercise Report for Experimental Study of Bubble Scrubbing in Water Coolant Pool

Nuclear Science and Engineering Division

ANL/NSE-25/31

Benchmark Exercise Report for Experimental Study of Bubble Scrubbing in Water Coolant Pool

Taeil Kim, Dong Hoon Kam, David Grabaskas
Nuclear Science and Engineering Division
Argonne National Laboratory

Kyle Becker, Mark Anderson
Department of Mechanical Engineering
University of Wisconsin-Madison

Jun 17, 2025

Abstract

Mechanistic assessments of radionuclide release during postulated accidents are expected to be included in advanced reactor license applications. The mechanistic source term (MST) provides an opportunity for vendors to realistically evaluate the radiological consequences of an incident, and may aid in justifying reduced emergency planning zones and plant sites. However, the development of MSTs for advanced nuclear reactors is challenging because there are numerous phenomena that can affect the transport and retention of radionuclides. As part of a trial MST assessment for a metal-fueled, pool-type sodium cooled fast reactor (SFR), led by Argonne National Laboratory, a simplified radionuclide transport code (SRT code) was developed, which includes models to estimate the quantity of fission product aerosols scrubbed in the sodium pool during postulated accident scenarios. In a pool-type SFR, when fission products are released into the coolant pool due to failure of fuel pins, most of the radionuclides are scrubbed by the coolant pool, but some have the potential to migrate to the cover gas region through entrainment within gas bubbles. The SRT code contains a model that evaluates this scrubbing behavior and calculates the fraction of fission product aerosols that reach the cover gas.

Due to a lack of available validation data for sodium pool scrubbing, the U.S. Department of Energy funded an experiment at the University of Wisconsin-Madison to measure aerosol scrubbing by injecting air bubbles containing aerosol into a coolant pool. Prior to performing an experiment with liquid sodium, a water loop experiment was performed. Their experiment evaluated the effect of changing the aerosol size, aerosol density, aerosol concentration, bubble size, and pool depth on the aerosol scrubbing efficiency of the pool. In this benchmark experiment, the base tests were conducted by repeated tests of isolated bubbles. Afterwards, more prototypic tests with bubble swarms were performed to evaluate the interactions between the bubbles. The bubble swarm test was able to confirm that a larger amount of aerosol scrubbing occurred than the single bubble test. It was also confirmed that as the bubble size, aerosol density, and pool height increase, the extent of pool scrubbing also increases and does not change with the aerosol concentration. In addition, since the degree of scrubbing is the lowest at aerosol sizes between 0.01 and 1 μm, that is, the largest amount of aerosol is emitted, it was confirmed that the analysis of this size in MST is the most important. This benchmark experiment informs the direction of future sodium experiments.

Table Of Contents

Figures

Tables

1 Introduction

The potential release of radioactive material during a postulated plant accident, referred to as the source term, is an important design metric and will be a primary focus of an advanced reactor licensing process. The U.S. Nuclear Regulatory Commission has stated that advanced reactor vendors are expected to present a mechanical assessment of the potential source terms when applying for their license applications [1]. The mechanistic source term (MST) can provide an opportunity for vendors to realistically evaluate the radiological consequences of an incident, reduce emergency planning areas and allow for smaller plant sites. However, the development of MSTs for advanced nuclear reactors is challenging, as there are numerous phenomena that often affect the transport and retention of radionuclides.

As part of a trial MST assessment for a metal-fueled, pool-type sodium cooled fast reactor (SFR) [1], led by Argonne National Laboratory, a simplified radionuclide transport (SRT) code was developed, which includes models to estimate the quantity of fission product aerosols scrubbed in the sodium pool during postulated accident scenarios. This SRT code models the release, transport, and retention of radionuclides in SFR and micro-reactor systems. SRT does not model the reactor's transient behavior, but utilizes the results of system analysis code or the analyst's postulated reactor conditions. Using this information, the SRT code evaluates several radionuclide behavioral phenomena, such as migration of radionuclides within fuel elements during irradiation, release of radionuclides from fuel in case of cladding failure, transport of radionuclides within reactor vessels and containment, and potential release into the environment.

In a postulated accident scenario, a failure of the fuel cladding would result in the release of fission products in the form of aerosols into the coolant pool. In both water-cooled reactors and sodium-cooled reactors, it is expected that most of these released aerosol particles are retained in the coolant pool [2, 3]. However, if aerosol particles become entrained in the gas bubbles when the cladding fails, they can be transported to the cover gas region without being scrubbed in the coolant pool. The amount of aerosols entering the pool divided by the amount of aerosol entering the cover gas is defined as the decontamination factor (DF). Once the radionuclides reach the area of the cover gas, transport outside the reactor system and facility is possible. In the development of the SFR's MST, these potential pathways for aerosol release were identified as a key knowledge gap through which radionuclides could be released into the environment.

Many studies have been conducted both experimentally and theoretically to better understand and quantify aerosol scrubbing during bubble transport in water-cooled reactors. Several aerosol scrubbing codes in water pools [4-6] have been developed based on the principles outlined by Fuchs [7]; the main methods of scrubbing utilized are gravitational sedimentation, inertial deposition, Brownian diffusion, and vapor condensation. Additionally, scrubbing codes have been implemented into fully integrated, engineering-level computer codes, such as MELCOR.

Much experimental work has been performed to complement these aerosol scrubbing codes. Kaneko et al. [8] conducted a parametric study analyzing the effects of key factors influencing pool scrubbing. Of the eight parameters studied (nozzle diameter, scrubbing depth, water and gas temperature, vapor fraction, gas velocity, gas pressure, particle density and diameter), scrubbing depth, particle diameter and gas vapor fraction were identified as the most important. Many other researchers have conducted similar experiments as Kaneko et al. did and found similar results [9-10]. Diao et al. [11] investigated the effect of gas jet orientation and showed that the gas injection direction affects the aerosol scrubbing efficiency significantly under the low inlet pressure condition. When the inlet pressure is higher than 0.3 MPa and gas flow state at nozzle exit is critical flow, the scrubbing efficiency is close to 100%, and the effect of gas injection direction is not obvious.

While many aerosol scrubbing studies have been conducted in water pools, there are not many aerosol scrubbing studies in sodium pools. Most notable, Miyahara et al. [12] studied mass transfer of iodine from a xenon-iodine mixed gas bubble to a sodium pool. In their experiments, the bubbles were generated by cracking the quartz ball at the bottom of a sodium pool. The rising velocity of the bubbles was determined from the signals of the sensors arranged vertically in the sodium pool. The bubbles reaching the sodium pool surface were collected in the inverted funnel and the collected gas containing sodium iodide aerosols was carried to a vacuum vessel through aerosol filters in the sampling system. Materials deposited on the filters, the inner surface of the funnel, the connected pipes and the vacuum vessel were dissolved in distilled water. The amount of iodine in the solution was then determined by the use of an inductively coupled plasma mass spectrometer. From their study, it was concluded that analysis based on mechanistic models is needed to more accurately predict fission product retention. Pradeep and Sharma [13] also developed a model for aerosol scrubbing in sodium pools. Their model was also based on the elimination methods described by Fuchs [7].

Becker and Anderson [14] built an experimental device at the University of Wisconsin-Madison to measure aerosol scrubbing by injecting air bubbles containing aerosols into the coolant pool. This benchmark experiment, funded by the U.S. Department of Energy, was performed to validate the theoretical model developed for the SRT code developed at Argonne National Laboratory with water [15]. While this model tracks radionuclide release through all potential pathways to the environment and models the entire source term in the event of a fuel pin failure, this benchmark experiment focused on the aerosol scrubbing via bubble transport, as presented by Bucknor et al. [16]. This aerosol scrubbing model is based on the principles of gravitational sedimentation, inertial deposition, Brownian diffusion, and sodium vapor condensation.

The purpose of this benchmark experiment is to conduct a sensitivity study to analyze the effect of various parameters such as bubbles size, aerosol concentration, aerosol particle size, aerosol density, and pool depths on the overall DF. This experiment performs DF tests on a single isolated bubble to provide a more accurate representation of the theoretical model and to provide a more direct comparison between the two. In addition to this, bubble shape and ascent rate were also recorded and compared to those found in the theoretical model. Afterwards, more prototypic tests with bubble swarms were performed to evaluate the interactions between the bubbles.

2 Experiment

2.1 Experimental Setup

Since the SRT code uses only the physical properties of fission products, a surrogate material was used instead of a radioactive material for safety reasons. Aluminum powder with an average weight diameter of 1 μm and nickel powder with an average weight diameter of 0.18 μm were used as surrogates to simulate fission products.

The aerosol was prepared using a SAG 410/U Solid Aerosol Generator manufactured by TOPAS. The SAG aerosol generator uses a rotating ring to deliver a constant and reproducible amount of powder [17]. This device is designed to inject aerosols at ambient pressure, so it is suitably modified to overcome the pressure head present at the point of injection into the water pool. The dosing system was separated from the electrical components and placed inside a pressure vessel. This pressure vessel was pressurized to a pressure 0.25 psi higher than the injection point, thereby eliminating backflow of the aerosols into the aerosol generator.

Additionally, because the SAG 410 was designed to operate continuously, it was necessary to use solenoid valves to pulse the device in such a way that it produced a single bubble that was accompanied by a relatively large amount of aerosols. Three solenoid valves were used for this purpose. The first solenoid valve controlled the inlet, the second solenoid valve controlled the outlet towards the spray nozzle, and the third one controlled the outlet vent needed to maximize the aerosol concentration of each bubble. The solenoid valve was controlled using an NI cRIO-9024 Real-Time controller. The NI cRIO was connected to a data acquisition computer using National Instruments LabVIEW 2019 to run the system and record temperature, pressure, and flow measurements.

The water pool was fabricated using a 19-cm ID and 2.45-m long polycarbonate tube. This diameter was used as recommended by Clift et al. [18] to achieve a ratio close to 1:8 for bubble size to tube diameter to limit the drag on the bubble imposed. The temperatures were measured using four type-K ungrounded thermocouple probes with 1.5875-mm diameter and a stated uncertainty of ± 2.2 °C. The first thermocouple was installed 16.5 cm above the nozzle and other thermocouples were installed at a distance of 60 cm. The thermocouples were inserted 1 cm into the water pool so as to not disrupt the bubble flow. This setup allowed temperature measurements at various points along the length of the water pool and within the cover gas region. An additional thermocouple was installed in the pressure vessel to ensure an isothermal setting. This happened naturally because the tests were run at room temperature (297K). Two Siemens SITRANS P410 pressure transmitters, with 0–30 psi gauge pressure range, were used to measure the pressures of the test setup. One was used to record the pressure in the pressure vessel and the second was used to record the pressure in the cover gas region.

Deionized water was used to limit impurities in the water. The air-aerosol mixture was then injected into the water pool using an inverted, cone nozzle. This allowed large bubbles to be produced with little to no bubble breakup.

A dilution cross flow of air was applied 7.5 cm above the water pool to carry the aerosols through the top collection system. This was necessary to decouple the bubble transport physics from the aerosol deposition mechanism that could occur if the aerosol was within the region of the cover gas. This new gas stream entrained by aerosol particles was captured using an inverted funnel. The gas flow is then passed through a coaxial mixer to further increase the gas flow to meet the specifications required by the particle sizer.

The gas flow rate was recorded using an Omega FMA6713 flow meter. And the sampling of the aerosol particles was conducted using a MOUDI ten-stage, rotating, cascade impactor. Inertial impactors function by classifying aerosols by their aerodynamic diameter. Impactors are governed primarily by Stokes number [19], defined by Eq. (1):

$$St = \frac{\rho_p C_s V_o D_p^2}{9\mu W}$$

where ρ_p is the particle density, C_s is the slip correction, V_o is the average velocity at nozzle exit, D_p is the particle diameter, μ is the air viscosity, and W is the nozzle diameter. This impactor allowed for particle sampling from sizes of 18 to 0.056 µm in incremental steps and the final filter allowed to trap additional aerosol particles. This allows the measurements of a wide range of aerosol sizes. A uniform deposit was obtained by rotating every other stage. Aerosol samples were collected using an aluminum foil substrate. To reduce solid particle bounce, each substrate was coated with an aerosolized silicone oil. Thereafter, the substrates were placed in a furnace at 150 °C for 3 h to eliminate volatility in substrate weight as recommended by Marple et al. [19]. The aluminum substrates were weighed prior to and after each test using a CPA26P Sartoruis microbalance. The balance had a readability of 2 μg and a repeatability of ±4 μg [20]. The entire experimental setup is shown in Figure 1.

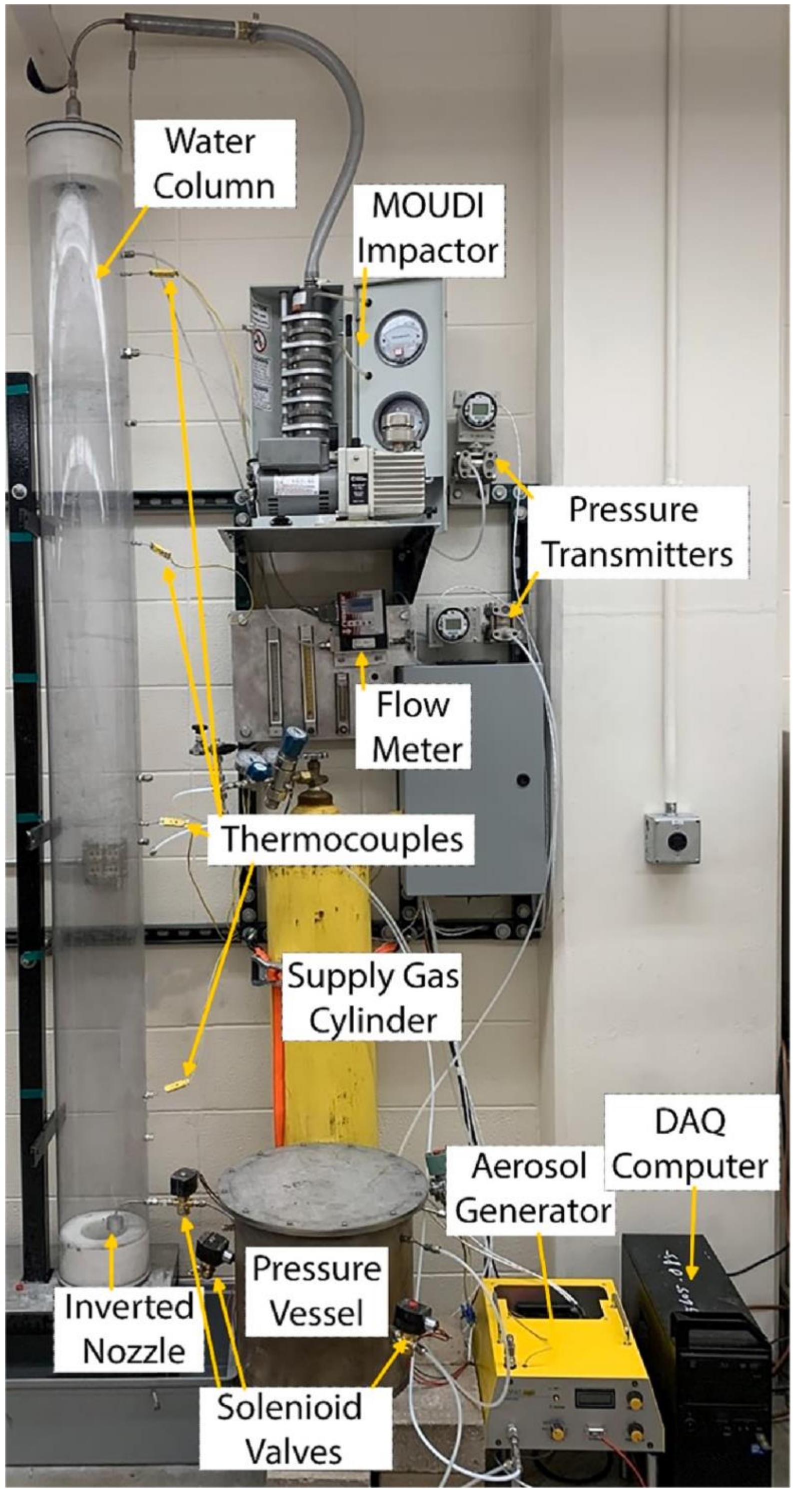

Figure 1. Experimental setup [14][1]

[1]This article was published in Nuclear Engineering and Design, Volume 377, K. Becker and M. Anderson, "Experimental study of SRT scrubbing model in water coolant pool," Article 111130, Copyright Elsevier (2021).

2.2 Experimental Methods and Parameters

Each test required three steps as follows: The first step was to perform a calibration of the impactor. The aerosol generator, under the same conditions as an ordinary run, was connected directly to the MOUDI impactor. This test allowed for quantification of the amount, and size distribution of aerosols being injected. The second step was to characterize any losses associated with collection. For this step, aerosols were injected into the empty water column at the height of the water–air interface expected for a typical experiment. This allowed for quantification of losses in the collection system. The third step was to run a scrubbing test. This involved injecting the aerosol-entrained bubble into the water column and measuring the amount of aerosols that passed through the water pool and calculating DF. All three steps were required per test for each condition to isolate scrubbing through the pool from other forms of loss (such as impaction on tubing, aerosol settling, etc.). In addition, for each experimental condition, five tests were run, each with 500 bubbles, to obtain an average DF with a reasonable uncertainty and to validate the reproducibility of the experiment.

Parameters of bubble size, aerosol size, aerosol density, aerosol concentration and pool depth were varied to investigate their effect on DF. The values of the parameters used in the experiments are summarized in Table 1.

In the experiments, tests with a single isolated bubble were performed as base tests to provide a more direct comparison with the SRT theoretical model representing isolated single bubbles. Then, tests with a bubble swarm were performed to evaluate the effect of the bubble swarm on the scrubbing. The assumption that a single, isolated bubble rising in a pool used in the SRT code was evaluated by comparing the results between the single bubble tests and the bubble swarm tests. A representative image of the bubble swarm is shown in Figure 2.

Table 1. Test parameters [14][2]

Parameters	Units	Values Tested			
Particle Size	μm	0.018-18			
Particle Density	g/cm^3	2.7 (aluminum)		8.9 (nickel)	
Bubble Size	cm	1.81	2.19	2.87	3.27
Aerosol Concentration	g/m^3	26.5		13.2	
Pool Depth	m	1.8		0.9	

[2]This article was published in Nuclear Engineering and Design, Volume 377, K. Becker and M. Anderson, “Experimental study of SRT scrubbing model in water coolant pool,” Article 111130, Copyright Elsevier (2021).

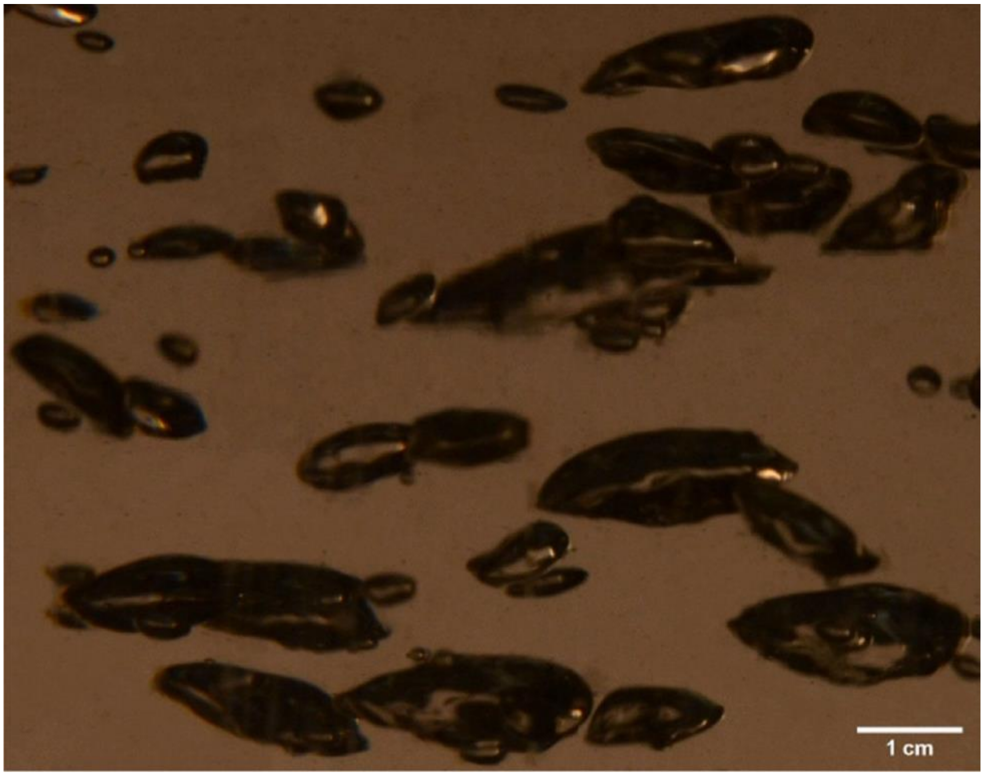

Figure 2. Representative image of bubble swarm [14][3]

[3]This article was published in Nuclear Engineering and Design, Volume 377, K. Becker and M. Anderson, "Experimental study of SRT scrubbing model in water coolant pool," Article 111130, Copyright Elsevier (2021).

3 Results

3.1 Single Bubble Experiments

First, the effect of particle size on DF was investigated by varying the particle size from 0.018 μm to 18 μm with the pool height of 6 feet, aerosol concentration of 26.5 mg/cm^3 (high aerosol concentration), aerosol density of 2.7 g/cm^3 (Al aerosols), and bubble diameter from 1.81 cm to 3.27 cm. The results are shown in Figure 3. In all experiments, DF decreased with increasing particle size at first, then it increased with increasing particle size. It can be attributed to the exponential increase in Brownian diffusion and inertial deposition with change in aerosol particle size. Due to Brownian diffusion for relatively small particles, due to inertial deposition for relatively large particles, relatively small and large particles are nearly entirely scrubbed. Gravity sedimentation also decreases with increasing bubble size, but is negligible compared to inertial deposition. From this, it can be said that both Brownian diffusion and inertial deposition are the two dominant scrubbing mechanisms for relatively small and large particles (larger than 1 μm, or less than 0.02 μm).

The effect of bubble size on DF was investigated by varying the equivalent diameter of the bubble. The results also can be seen in Figure 3. It was shown that DF decreased as bubble size (bubble diameter) increased. This is likely because the aerosols are relatively more scrubbed with small bubbles, as the surface area to volume ratio of the bubbles decreases with increasing bubble size. In addition to this, as the bubble size increases, the rise velocity also increases, so the time for bubble scrubbing is reduced, which leads to a lower DF as the bubble size increases.

The spread of relatively important particle sizes (particle sizes with a DF of less than 10), is increased with increasing bubble sizes. This can be attributed to the Brownian diffusion and inertial deposition scrubbing rates increasing at a slower rate with increasing bubble sizes.

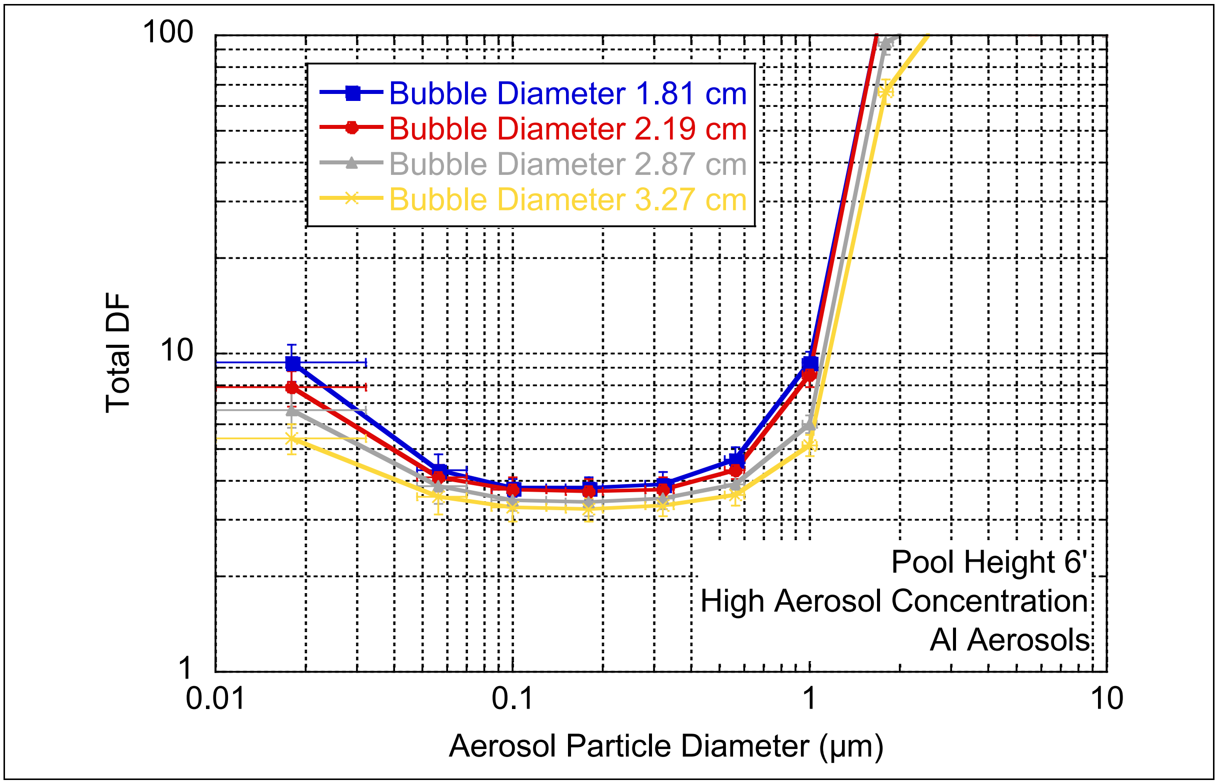

Figure 3. Relationship between aerosol particle size and DF for various bubble sizes

Second, the effect of aerosol density on DF was investigated by using different powders: aluminum powders (ρ_{Al} = 2.7g/cm^3) and nickel powders (ρ_{Ni} = 8.9g/cm^3). These experiments were conducted with the pool height of 6 feet, high aerosol concentration, and bubble diameter of 2.87 cm. The relationship between the aerosol particle size and DF for different aerosol densities is shown in Figure 4. Again, for both particle types, DF decreased with increasing particle size at first, then it increased with increasing particle size.

It was found that the particles with higher densities experience more scrubbing for relatively particle sizes greater than 0.1 μm and that scrubbing becomes independent of aerosol density for relatively small aerosols. This is because Brownian diffusion is independent of aerosol density, whereas gravitational sedimentation and inertial deposition both increase exponentially with aerosol density.

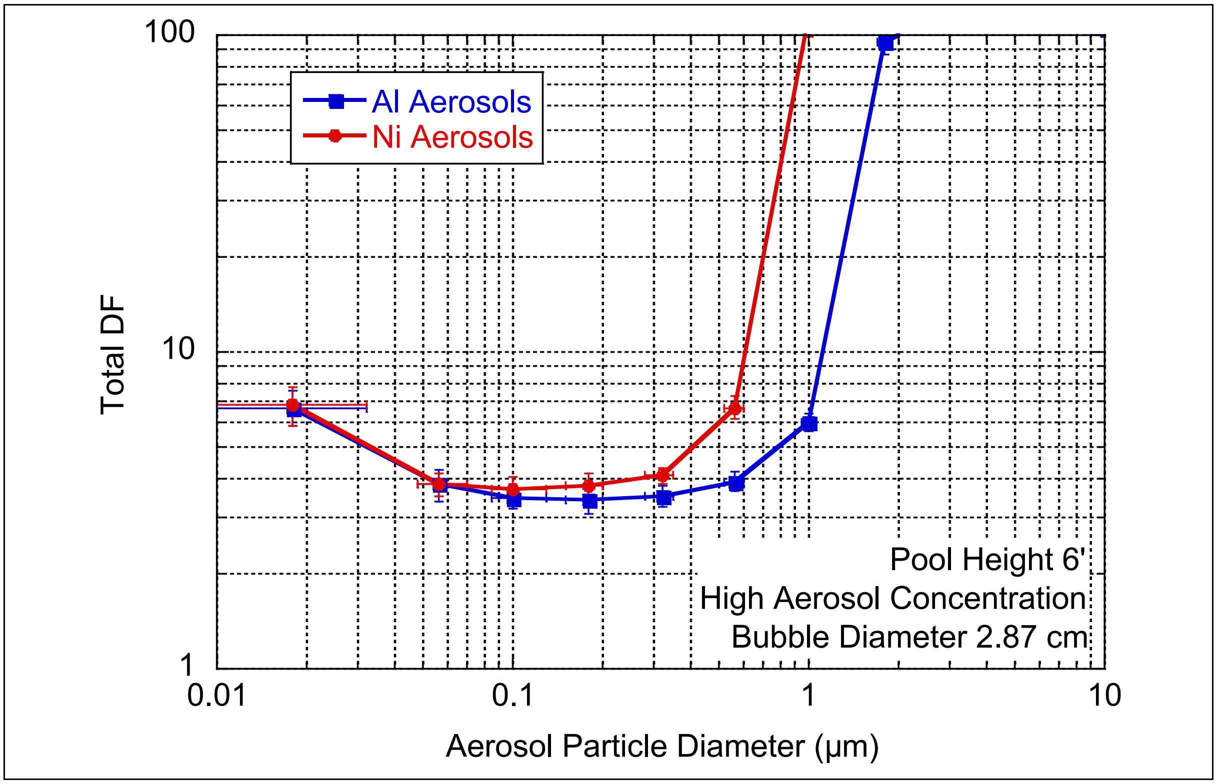

Figure 4. Relationship between aerosol particle size and DF for different particle densities

Third, a series of tests were conducted to investigate the effects of pool height on the DF with the high aerosol concentration, Al aerosols, and bubble diameter of 2.87 cm. The relationship between the aerosol particle size and DF for different pool heights is shown in Figure 5. Same as previous tests series, similar trends in DF with aerosol particle size were found for both pool heights. DF decreased with increasing particle size at first, then it increased with increasing particle size.

It was found that DF increased with increasing pool height. It can be inferred that the greater the pool height, the greater the particle scrubbing due to the increased residence time for scrubbing to occur.

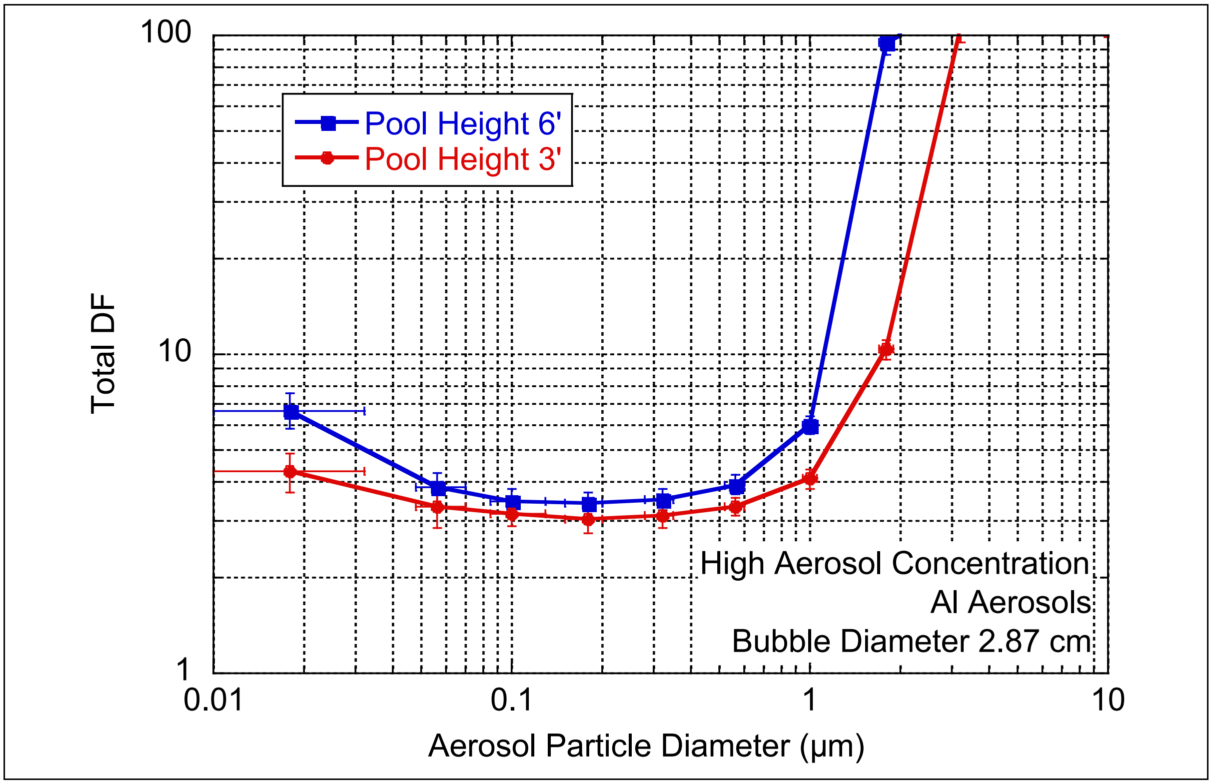

Figure 5. Relationship between aerosol particle size and DF for different pool heights

A fourth experimental series of tests was conducted to study the effects of aerosol concentration on the DF with the pool height of 6 feet, Al aerosols, and bubble diameter of 2.87 cm. The relationship between the aerosol particle size and DF for different aerosol concentrations is shown in Figure 6.

Similarly, the results showed that DF decreased with increasing particle size at first, then it increased with increasing particle size for both aerosol concentrations. And the experimental data showed that almost no change in DF with the change of aerosol concentration.

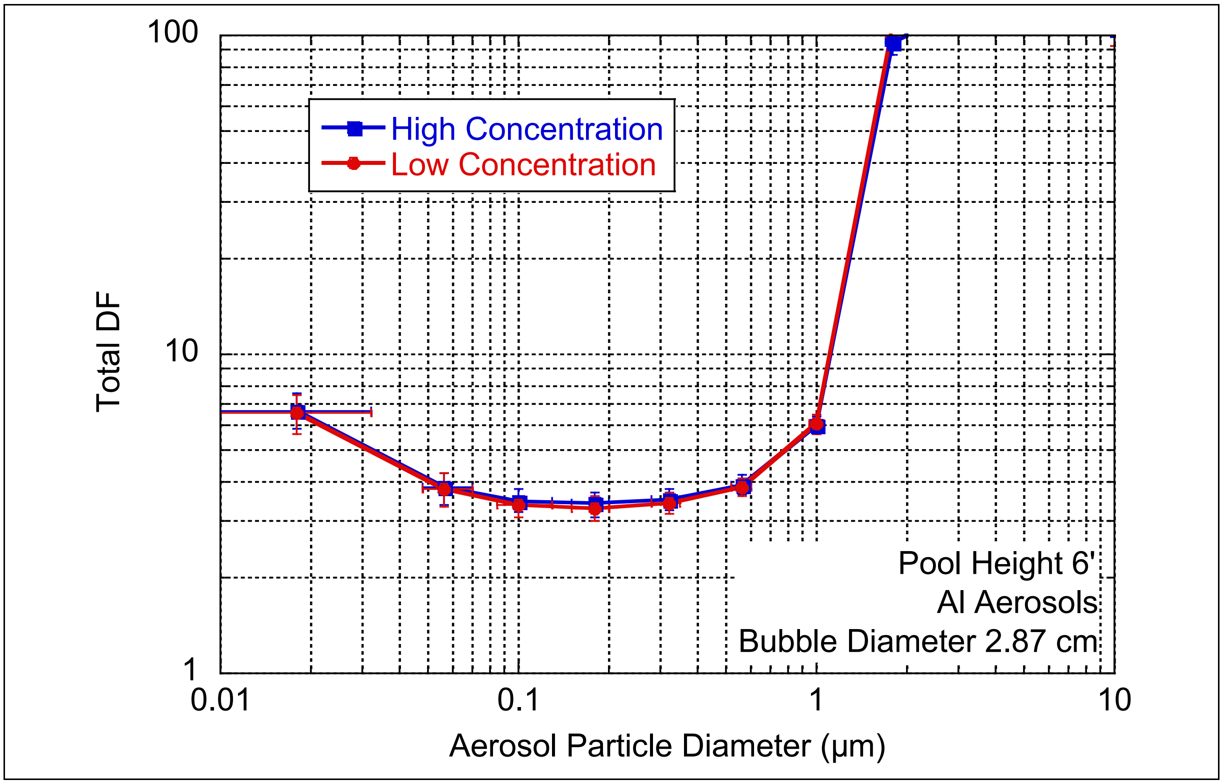

Figure 6. Relationship between aerosol particle size and DF for different aerosol concentrations

3.2 Bubble Swarm Experiments

Abe et al. found that the bubble swarm more accurately models the expected behavior following a fuel pin failure [21]. Therefore, a set of tests was performed using a bubble swarm with the pool height of 6 feet, high aerosol concentration, and Al aerosols. The results were compared with the experimental results using a single isolated bubble.

The bubble swarm was generated by passing the inlet gas flow through a sparging device. To characterize the bubble size in this experiment, an average bubble size was used to represent the distribution of bubble sizes generated. From analysis of the high-speed imagery, it was found the average bubble size was 0.984 *cm* with a standard deviation of 0.736 *cm*.

The relationship between the aerosol particle size and DF from the bubble swarm tests is shown in Figure 7. Same as the single bubble tests, DF decreased with increasing particle size at first, then it increased with increasing particle size for the bubble swarm tests. However, there is an increased shift to higher DF seen in these bubble swarm experiments. This can be attributed to the bubble-to-bubble interactions (such as coalescence) along with the added turbulent nature of the flow.

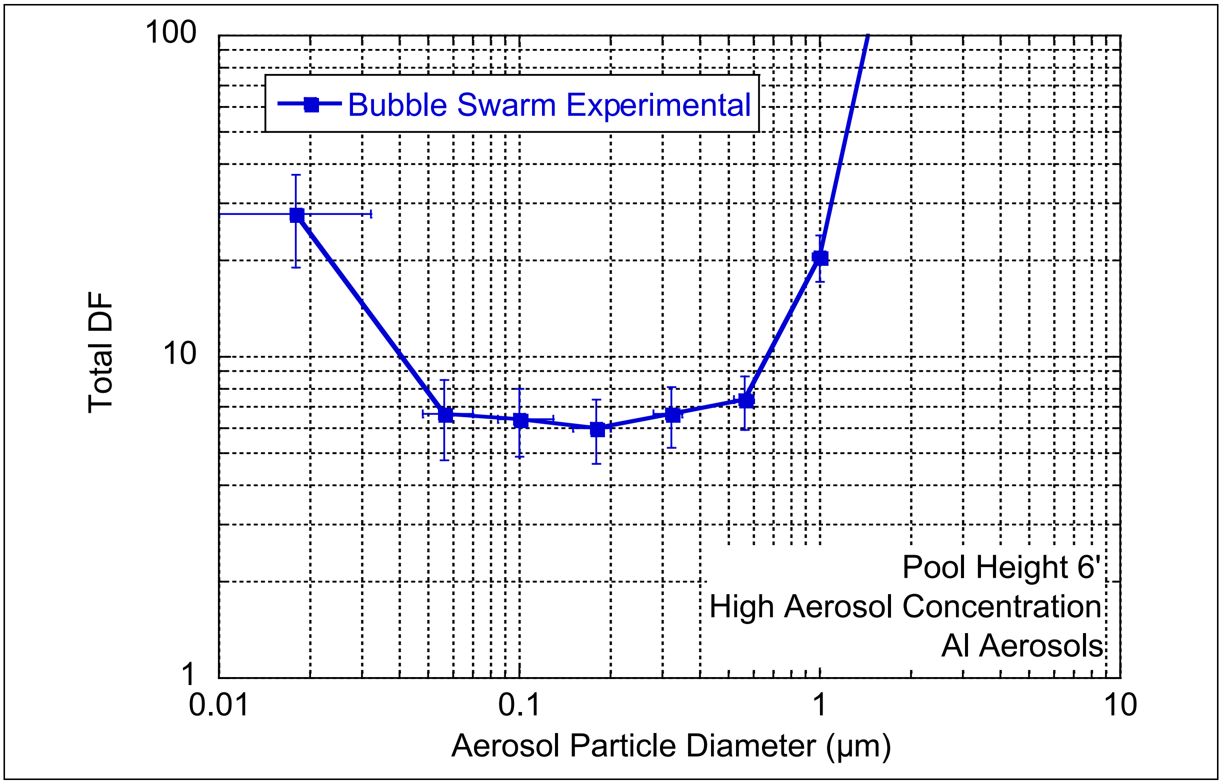

Figure 7. Relationship between aerosol particle size and DF from bubble swarm tests

4 Conclusion

The University of Wisconsin [14] successfully conducted a water-loop experiment of aerosol scrubbing for the assessment of the SRT MST code presented by Grabaskas and Bucknor [15, 16]. The effects of bubble size, aerosol density, pool depth, and aerosol concentration on DF were all analyzed for a wide range of aerosol sizes.

In all experiments, DF decreased with increasing particle size at first, then it increased with increasing particle size. It can be attributed to the exponential increase in Brownian diffusion and inertial deposition with change in aerosol particle size. The degree of scrubbing is the lowest at aerosol sizes between 0.01 and 1 μm, that is, the largest amount of aerosol is transported.

First, it was shown that DF decreased as bubble size (bubble diameter) increased. This is likely because the aerosols are relatively more scrubbed with small bubbles, as the surface area to volume ratio of the bubbles decreases with increasing bubble size. In addition to this, as the bubble size increases, the rise velocity also increases, so the time for bubble scrubbing is reduced, which leads to a lower DF as the bubble size increases. Second, it was found that the particles with higher densities experience more scrubbing for relatively particle sizes greater than 0.1 μm and that scrubbing becomes independent of aerosol density for relatively small aerosols. This is because Brownian diffusion is independent of aerosol density, whereas gravitational sedimentation and inertial deposition both increase exponentially with aerosol density. Third, it was found that DF increased with increasing pool height. It can be inferred that the greater the pool height, the greater the particle scrubbing due to the increased residence time for scrubbing to occur. Fourth, the experimental data showed that almost no change in DF with the change of aerosol concentration.

In addition, a comparison of pool scrubbing from a bubble swarm to that of the model, which was developed to model a single, isolated bubble, was conducted to analyze the simplification used in the code. From this comparison, it was found that further pool scrubbing occurs when bubbles interact with one another and higher gas flows are induced, resulting in turbulent flows.

Future experiments in sodium pools of similar conditions and geometries are needed in order to further validate the SRT code. For the upcoming sodium pool experiment, pool temperatures will be added to the test parameters. This experiment will allow for a more direct comparison of experimental data with that found in the native SRT code without code modifications.

REFERENCE

1. D. Grabaskas, M. Bucknor, J. Jerden, A. Brunett, M. Denman, A. Clark, and R. Denning, "Regulatory technology development plan - sodium fast reactor: mechanistic source term development - trial calculation," Argonne National Laboratory, ANL-ART-49, 2016.
2. H. Allelein, A. Auvinen, J. Ball, S. Guentay, L. Herranz, A. Hidaka, A. Jones, M. Kissane, D. Powers, and G. Weber, "State-of-the-art report on nuclear aerosols," Nuclear Energy Agency, NEA/CSNI/R(2009)5, 2009.
3. D. Grabaskas, A. Brunett, M. Bucknor, J. Sienicki, and T. Sofu, "regulatory technology development plan - sodium fast reactor: mechanistic source term development," Argonne National Laboratory, ANL-ART-3, 2015.
4. A. Wassel, A. Mills, D. Bugby, and R. Oehlberg "Analysis of radionuclide retention in water pools," Nucl. Eng. Des., 90(1), pp. 87–104, 1985.
5. D. Powers and J. Sprung, "A simplified model of aerosol scrubbing by a water pool overlying core debris interacting with concrete," Sandia National Laboratories, NUREG/CR-5901, 1993.
6. T. Kanai, M. Furuya, T. Arai and Y. Nishi, "Development of an aerosol decontamination factor evaluation method using an aerosol spectrometer," Nucl. Eng. Des., 303, pp. 58–67, 2016.
7. N. Fuchs, "The mechanics of aerosols," Pergamon Press, 1964.
8. I. Kaneko, M. Fukasawa, M. Naito, K. Miyata, and M. Matsumoto, "Experimental study on aerosol removal effect by pool scrubbing," 22nd DOE/NRC Nuclear Air Cleaning and Treatment Conference, Denver, United States, 1992.
9. A. Dehbi, D. Suckow, and S. Guentay, "Aerosol retention in low-subcooling pools under realistic accident conditions," Nucl. Eng. Des. 203(2-3), pp. 229–241, 2001.
10. Y. Li, Z. Sun, H. Gu, and Y. Zhou, "Deposition characteristic of micro-nano soluble aerosol under bubble scrubbing condition," Ann. Nucl. Energy, 133, pp. 881–888, 2019.
11. H. Diao, Y. Zhou, H. Gu, Y. Li, and C. Yan, "Experimental study on the scrubbing efficiency of aerosols contained in horizontal and vertically downward submerged gas jet," Prog. Nucl. Energy, 126, Article 103406, 2020.
12. S. Miyahara, N. Sagawa, and K. Shimoyama, "Iodine mass transfer from xenon-iodine mixed gas bubble to liquid sodium pool," J. Nucl. Sci. Technol., 33(2), pp. 128–133, 1996.
13. A. Pradeep and A. Sharma, "Semi-empirical model for wet scrubbing of bubble rising in liquid pool of sodium-cooled fast reactor," Nucl. Eng. Technol., 50(6), pp. 849–853, 2018.
14. K. Becker and M. Anderson, "Experimental study of SRT scrubbing model in water coolant pool," Nucl. Eng. Des., 377, Article 111130, 2021.
15. D. Grabaskas, M. Bucknor, and J. Jerden, "Simplified Radionuclide Transport (SRT) code: user's manual," Argonne National Laboratory, ANL-SRT-4, Rev 2.0.1, 2020.
16. M. Bucknor, M. Farmer, and D. Grabaskas, "An assessment of fission product scrubbing in sodium pools following a core damage event in a sodium cooled fast reactor," International

Conference on Fast Reactors and Related Fuel Cycles: Next Generation Nuclear Systems for Sustainable Development (FR 17), Yekaterinburg, Russia, 2017.

17. SAG 410, Dosing Range 0.5mg/h up to 6kg/h. (n.d.). TOPAS. Retrieved July 7, 2020, from https://www.topas-gmbh.de/en/produkte/sag-410/.
18. R. Clift, J. Grace, and M. Webber, “Bubbles, drops, and particles,” Courier Corporation, 2005.
19. V. Marple, K. Rubow, and S. Behm, “A micro-orifice uniform deposit impactor (MOUDI): description, calibration, and use,” Aerosol Sci. Technol., 14(4), pp. 434–446, 1991.
20. Sartorius CPA26P Microbalance. (n.d.). Sartorius. Retrieved July 9, 2020, from https://scaleman.com/micro-balance-weighing-sartorius-cpa26p.html.
21. Y. Abe, K. Fujiwara, S. Saito, T. Yuasa, and A. Kaneko, “Bubble dynamics with aerosol during pool scrubbing,” Nucl. Eng. Des., 337, pp. 96–107, 2018.

APPENDIX

- Parametric uncertainty table

Bubble diameter		**Pool depth**	
Mean[cm]	Uncertainty[cm]	Mean[m]	Uncertainty[m]
1.81	0.19	1.83	0.0127
2.19	0.21	0.91	0.0127
2.87	0.28	-	
3.27	0.34		
0.984 (swarm)	0.736		

- Aerosol size uncertainty table

Aerosol particle size		
Mean [μm]	Minus	Plus
18	6	4
10	1.25	0.5
5.6	0.6	0.4
3.2	0.1	0.1
1.8	0.1	0.1
1	0.05	0.05
0.56	0.04	0.04
0.32	0.04	0.03
0.18	0.03	0.02
0.1	0.015	0.03
0.056	0.008	0.014
0.018	0.008	0.014

Nuclear Science Engineering Division
Argonne National Laboratory
9700 South Cass Avenue, Bldg. 208
Argonne, IL 60439-4842

www.anl.gov